Orbital and spin moments in $SmFe_2$ studied by means of white-x-ray magnetic diffraction

2002 J. Phys.: Condens. Matter 14 9525

(http://iopscience.iop.org/0953-8984/14/41/309)

INSTITUTE OF PHYSICS PUBLISHING JOURNAL OF PHYSICS: CONDENSED MATTER

J. Phys.: Condens. Matter **14** (2002) 9525–9534 PII: S0953-8984(02)29524-7

Orbital and spin moments in $SmFe_2$ studied by means of white-x-ray magnetic diffraction

Hayato Miyagawa[1], Tetsuya Nakamura[1], Yasuhiro Watanabe[1], Masahisa Ito[2], Hiromichi Adachi[3], Hiroshi Kawata[3] and Susumu Nanao[1]

[1] Institute of Industrial Science, University of Tokyo, 4-6-1 Komaba, Meguro-ku, Tokyo 153-8505, Japan
[2] Faculty of Science, Himeji Institute of Technology, 3-2-1 Kouto, Kamigori, Ako-gun, Hyogo 678-1297, Japan
[3] Photon Factory (PF), Institute of Materials Structure Science, 1-1 Oho, Tsukuba, Ibaraki 305-0801, Japan

E-mail: miyagawa@iis.u-tokyo.ac.jp

Received 8 October 2001, in final form 12 August 2002
Published 4 October 2002
Online at stacks.iop.org/JPhysCM/14/9525

Abstract

A magnetic structure of $SmFe_2$ with a Laves phase crystalline structure was investigated by means of white-x-ray magnetic diffraction. The orbital and the spin magnetic form factors of Sm and Fe ions have been obtained as a function of momentum transfer. Their extrapolation to zero momentum transfer, according to the dipole approximation based on an atomic model, has given the values of the spin and the orbital magnetic moments of Sm ions as $-2.54 \pm 0.55\ \mu_B$ and $2.79 \pm 0.61\ \mu_B$, respectively. This result confirms that the small magnetic moment of Sm ions arises from antiparallel coupling between the spin and the orbital magnetic moments. The spin and the orbital magnetic moments of Fe ions have been also estimated, as $1.13 \pm 0.25\ \mu_B$ and $0.19 \pm 0.04\ \mu_B$, respectively.

1. Introduction

For the last two decades, x-ray magnetic scattering experiments have been developed as powerful tools for studies of magnetism. Highly brilliant synchrotron radiation sources have extended the scope of the applications of x-ray studies to many and various magnetic materials. Thanks to the intense x-rays, it has also become possible to measure x-ray magnetic scattering amplitude quantitatively; this is much smaller than that of the normal charge scattering—by of the order of $\hbar\omega/mc^2$ [1–3]. The most remarkable aspect of the x-ray magnetic scattering technique is that the spin and the orbital magnetic form factors can be separated; we will call this S–L separation [3–6], because the cross-section of the non-resonant magnetic Bragg scattering has independent spin and orbital terms of the magnetic form factors. The white-x-ray magnetic diffraction (WXMD) technique proposed by Collins and Laundy [14] enables

us to carry out the S–L separation without using complicated experimental procedures. For WXMD, the following simple equation can be applied when polarized x-rays are scattered with the scattering angle (2θ) of 90°:

$$R = \frac{I_+ - I_-}{I_+ + I_-} = \frac{E}{mc^2} f_P \left[\frac{2S(k)}{n(k)} \sin\alpha + \frac{L(k)}{n(k)} (\sin\alpha + \cos\alpha) \right]. \tag{1}$$

Here, I_+ and I_- are the diffraction intensities for the positive and the negative directions of a sample's magnetization, respectively; E is the incident x-ray energy; mc^2 is the electron rest mass energy; f_P is the polarization factor which is equal to $p_c/(1 - p_l)$, where p_c and p_l are the degrees of circular polarization and linear polarization in the scattering plane, respectively. $S(k)$, $L(k)$, and $n(k)$ are the structure factors of the densities of the spin magnetic moment, the orbital magnetic moment, and the electron charge, respectively. α is the angle between the directions of the incident x-rays and the magnetization of the specimen. Flipping ratio R corresponds to the magnetic scattering amplitude. This equation indicates that $S(k)/n(k)$ and $L(k)/n(k)$, which have coefficients depending on α, can be evaluated separately from pairs of R-values obtained for two different α-values. The advantages of the WXMD technique have been reported in [14–17]. Several WXMD experiments have been attempted previously on pure metals, Fe [15–18], Ni [17], Co [19], Tb [20], and some other compounds [5, 16]. WXMD studies of 3d–4f intermetallic compounds have also been reported, for $HoFe_2$ [15] and $DyCo_5$ [21]. Good agreement of the magnetic form factors between WXMD study, neutron study, and theoretical calculations has already been confirmed for $HoFe_2$ [16].

In the present study, a WXMD study of $SmFe_2$ was performed in order to deduce the spin and the orbital magnetic form factors. $SmFe_2$ is an intermetallic compound and has the cubic Laves phase of C15 structure. The magnetic moment of $SmFe_2$ at 4.2 K and the Curie temperature of a polycrystalline sample have been reported as 2.25–2.75 μ_B per formula unit and 676 K, respectively [22–24]. For a single-crystal sample, the magnetic moment has been obtained as 3.02 μ_B per formula unit [25]. The magnetic moments of the Fe sublattice in RFe_2 (R: rare earth) [8, 9], excluding $SmFe_2$, have been estimated as from 1.4 to 2.0 μ_B by means of nuclear magnetic resonance measurements. Therefore, the magnitude of the magnetic moments of Sm ions is considered to be very small. It has been believed that such a small value of the magnetization is due to antiparallel coupling between the spin magnetic moment and the orbital one, which reduces the moment at Sm sites. The details of the magnetic structure are, however, unknown, because neutron diffraction experiments are difficult for Sm compounds [28]; this is because Sm is one of the neutron absorption atoms. In the present study of WXMD, the spin and the orbital magnetic form factors of both Sm and Fe atoms at room temperature have been deduced from the experimental data with an analysis using the dipole approximation. The net spin and the orbital moments have been estimated as the values of $S(0)$ and $L(0)$, where $S(0)$ and $L(0)$ are $S(k)$ and $L(k)$ at $k = 0$.

2. Experimental details

A single crystal of $SmFe_2$ was synthesized by the Bridgman method, where a $Sm_{65}Fe_{35}$ (at.%) alloy ingot was used as a base material. The $Sm_{65}Fe_{35}$ ingot was prepared by arc-melting from Sm (purity: 99.9%) and Fe (99.9%) metals in an argon gas atmosphere. The ingot was placed in an alumina crucible coated with a boron nitride layer. The crucible was packed in a quartz ampoule with Ar gas (150 Torr) and was moved down slowly in a furnace after annealing for 4 h at 850 °C. The specimen of the single crystal has the dimensions of roughly 2 mm diameter × 0.1 mm thickness and has a (1 1 1) plane in the disc surface.

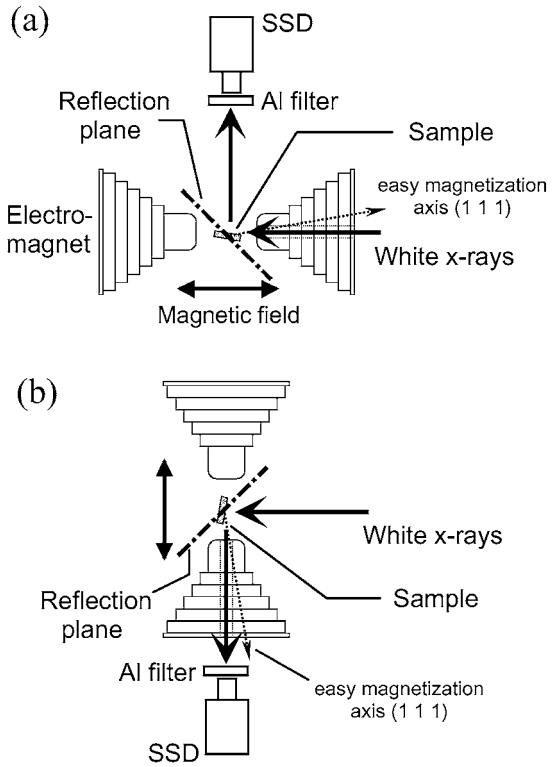

Figure 1. The schematic geometry of the x-ray magnetic Bragg scattering measurement. The angle α between the directions of the incident x-rays and the magnetization of the sample is set to (a) 0° and (b) 90°.

The magnetic field dependence of the magnetization was measured using a vibrating-sample magnetometer. The reflection planes (h h 0) and ($3h$ $3h$ h) have been chosen as possible configurations such that the easy magnetization axis should be very close to the direction of the magnetic field applied to the sample, because the present analysis will be carried out on the assumption that the angle α can be given as the angle between the directions of the incident x-rays and an external magnetic field instead of the magnetization of the sample. The angles between the easy magnetization axes (1 1 1) and the direction of the applied field are 9.8° in the experiment on the (h h 0) reflection planes series and 3.5° in the experiment on the ($3h$ $3h$ h) series. The saturation of the sample magnetization for each case is verified by magnetization measurements using a vibrating-sample magnetometer.

The measurement of the WXMD at room temperature was carried out at $BL3C_2$ at the Photon Factory, Institute of Material Structure Science, where a diffractometer designed for WXMD experiments is installed. Schematic layouts for the experimental devices with $\alpha = 0°$ and 90° are shown in figures 1(a) and (b). The geometries with $\alpha = 0°$ and 90° give $L(k)$ and $L(k)+2S(k)$ according to equation (1), respectively. The sample was mounted in a field of 1 T created by an electromagnet. A pure germanium solid-state detector (SSD) in which the energy resolution is better than 300 eV was used to count the intensities of the scattered x-rays. In the case where the energy separation between the fluorescence and the diffraction was too small to resolve by means of the SSD, high-energy-resolution measurements were performed using an analyser crystal of graphite (0 0 2). The direction of the external magnetic field applied to the

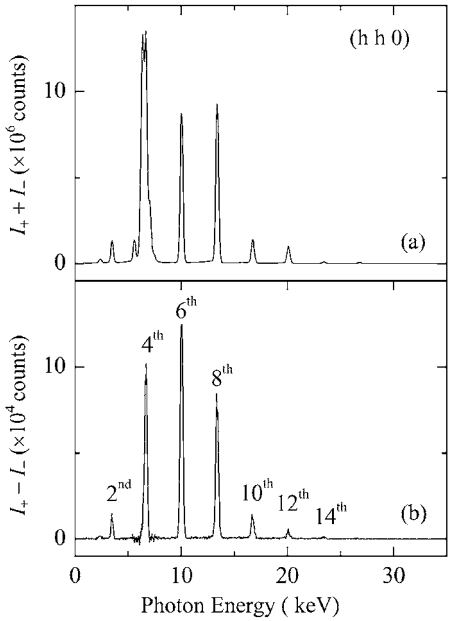

Figure 2. Typical profiles of (h h 0) reflections at $\alpha = 0°$. (a) The profile of charge scattering. (b) The profile of magnetic scattering. The diffraction peaks up to $h = 22$ were used for the analysis; the labels for the peaks from $h = 16$ to 22 are omitted.

sample was reversed every 10 s. The primitive level, which corresponds to the orbital plane of the synchrotron ring, was calibrated every 4 h in order to keep the polarization factor at the sample position constant during the measurements. The primitive level is the one which gives the minimum of the scattering intensities, because the scattering amplitude increases with the degree of circular polarization. The use of the white x-rays and single crystals often allows multiple-scattering paths. The multiple-scattering amplitudes were removed or minimized using an azimuthal scan.

3. Results and discussion

Typical diffraction patterns for the (h h 0) reflection are shown in figures 2(a) and (b), which correspond to the diffraction patterns of the charge ($I_+ + I_-$) and the magnetic scattering ($I_+ - I_-$), respectively. All the peaks in figure 2(a) are observed at the same time by means of an energy-dispersive measurement using an SSD. The (4 4 0) diffraction peak in figure 2(a) is superposed on three or four peaks of fluorescence lines such as Fe K$\alpha_{1,2}$ and Fe Kβ. In ($3h$ $3h$ h) reflections, the (3 3 1) peak is also superposed on the fluorescence. For (4 4 0), a high-energy-resolution measurement using an analyser crystal of a graphite (0 0 2) was performed, and the intensity of the diffraction peaks that are not contaminated by the fluorescence have been measured and used for analysis. The magnetic effects from these fluorescence peaks are negligible in figure 2(b), because their intensity can be accounted for as the area of magnetic circular dichroism in both the resonant and non-resonant energy regions of absorption. This means that the profile in figure 2(b) comes from just the magnetic effect of diffraction. The R-values measured for a series of (h h 0) reflections with $\alpha = 0°$ and 90° are plotted in figures 3(a) and (b), respectively; the R-values for the ($3h$ $3h$ h) series with $\alpha = 0°$ and

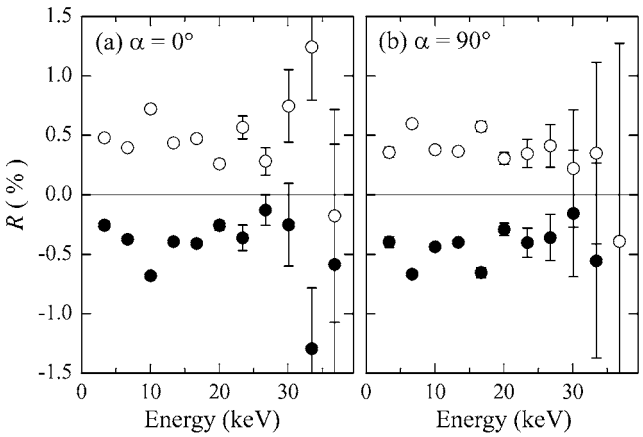

Figure 3. The flipping ratio R for the reflections of the (h h 0) series; (a) is for $\alpha = 0°$; (b) is for $\alpha = 90°$. The open circles denote the values measured by setting the sample position 0.5 mm below the orbital plane; the filled circles are for a position 0.5 mm above. The filled circle for (22 22 0) at 36.78 keV in panel (b) is not seen, because its value is 4.04 ± 1.90%.

90° are also plotted in figures 4(a) and (b), respectively. The open circles and the filled ones correspond to the values measured by setting the sample position at 0.5 mm below and above the orbital plane, respectively. The distributions of the plotted points in both figures 3 and 4 are favourably symmetric with respect to the primitive line of $R = 0$, which results from the antisymmetrical shape of f_P with respect to the orbital plane and ensures reliability of the present results. The averages of the absolute values of R obtained above and below the orbital plane are used for the analysis of the S–L separation based on equation (1). The values of f_P are tabulated in table 1; they were calculated with the computer program 'SPECTRA' using WXMD data measured for an iron single crystal in advance. The deduced $L(k)$, $S(k)$, and $L(k) + 2S(k)$ for both the (h h 0) and the ($3h$ $3h$ h) reflections are shown in figure 5. The structure factors of $F(k)$, $S(k)$, and $L(k)$ are given as

$$F(k) = N_{\mathrm{Sm}}(h,k,l)\,f_{\mathrm{Sm}}(k) + N_{\mathrm{Fe}}(h,k,l)\,f_{\mathrm{Fe}}(k), \tag{2}$$

$$S(k) = N_{\mathrm{Sm}}(h,k,l)S_{\mathrm{Sm}}(k) + N_{\mathrm{Fe}}(h,k,l)S_{\mathrm{Fe}}(k), \tag{3}$$

$$L(k) = N_{\mathrm{Sm}}(h,k,l)L_{\mathrm{Sm}}(k) + N_{\mathrm{Fe}}(h,k,l)L_{\mathrm{Fe}}(k), \tag{4}$$

where $f_{\mathrm{Sm}}(k)$ and $f_{\mathrm{Fe}}(k)$ represent the charge scattering form factors, $S_{\mathrm{Sm}}(k)$ and $S_{\mathrm{Fe}}(k)$ are the spin magnetic form factors, and $L_{\mathrm{Sm}}(k)$ and $L_{\mathrm{Fe}}(k)$ are the orbital magnetic form factors for Sm and Fe, respectively. The phase terms of the x-ray scattering for Sm and Fe sites are represented by N_{Sm} and N_{Fe}, respectively. The values of N_{Sm} and N_{Fe} for the (h h 0) and the ($3h$ $3h$ h) reflections are shown in table 1. Table 1 shows that $S(k)$ and $L(k)$ for the (h h 0) reflection series directly correspond to $S_{\mathrm{Sm}}(k)$ and $L_{\mathrm{Sm}}(k)$ in the case of $h = 4n + 2$, where n denotes an integer.

To deduce the values of the spin and the orbital moments from $S(k)$ and $L(k)$, an analysis using the dipole approximation based on a free ion model was carried out. According to the dipole approximation, the magnetic form factors are expressed as follows [31]:

$$S_{\mathrm{M}}(k) = S_{\mathrm{M}}(0)\langle j_0\rangle_{\mathrm{M}} \qquad (\mathrm{M} = \mathrm{Fe\ or\ Sm}) \tag{5}$$

$$L_{\mathrm{M}}(k) = L_{\mathrm{M}}(0)\{\langle j_0\rangle_{\mathrm{M}} + \langle j_2\rangle_{\mathrm{M}}\} \qquad (\mathrm{M} = \mathrm{Fe\ or\ Sm}). \tag{6}$$

Here, $S_{\mathrm{M}}(0)$ and $L_{\mathrm{M}}(0)$ correspond to the net spin and orbital magnetic moments, S_{M} and L_{M}, respectively, along with the applied magnetic field; $\langle j_0\rangle_{\mathrm{M}}$ and $\langle j_2\rangle_{\mathrm{M}}$ are the relativistic

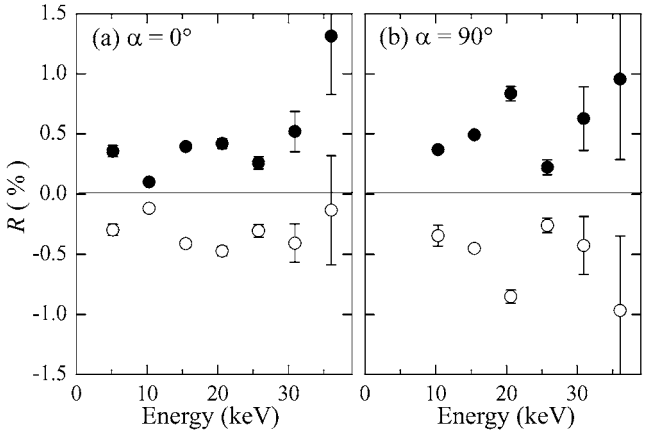

Figure 4. The flipping ratio R for the reflections of the ($3h$ $3h$ h) series; (a) is for $\alpha = 0°$; (b) is for $\alpha = 90°$. The open circles denote the values measured by setting the sample position 0.5 mm below the orbital plane; the filled circles are for a position 0.5 mm above. The filled and open circles for (3 3 1) at 5.153 keV in panel (b) are not seen, because their values are 2.48 ± 0.08 and $-2.66 \pm 0.10\%$, respectively.

Table 1. The polarization factor, f_P, and the phase terms, N_{Sm} and N_{Fe}, in the structure factors for the (h h 0) and ($3h$ $3h$ h) reflection series of $SmFe_2$ (h represents a natural number). The value of f_P has been calculated using WXMD data measured for an iron single crystal.

Index	f_P	N_{Sm}	N_{Fe}
(h h 0) $h \neq 2n$	—	0	0
(2 2 0)	12.06	8	0
(4 4 0)	11.17	8	16
(6 6 0)	10.80	8	0
(8 8 0)	10.59	8	16
(10 10 0)	10.40	8	0
(12 12 0)	10.56	8	16
(14 14 0)	10.42	8	0
(16 16 0)	10.42	8	16
(18 18 0)	10.41	8	0
(20 20 0)	10.41	8	16
(22 22 0)	10.41	8	0
(3 3 1)	11.45	5.66	−8
(6 6 2)	10.77	0	16
(9 9 3)	10.40	−5.66	−8
(12 12 4)	10.51	−8	16
(15 15 5)	10.42	−5.66	−8
(18 18 6)	10.41	0	16
(21 21 7)	10.41	5.66	−8
(24 24 8)	10.43	8	16

radial integrals of the product of the wavefunction multiplied by spherical Bessel functions of order 0 and 2, respectively. S_{Sm}, L_{Sm}, S_{Fe}, L_{Fe} are obtained as the best-fitted parameters by the least-squares method, where the weights of statistical errors are taken into account. All the reliable values of R up to (22 22 0) for the (h h 0) reflection series and up to (21 21 7) for the ($3h$ $3h$ 0) series except for (2 2 0) and (3 3 1) are used for the fitting analysis. The

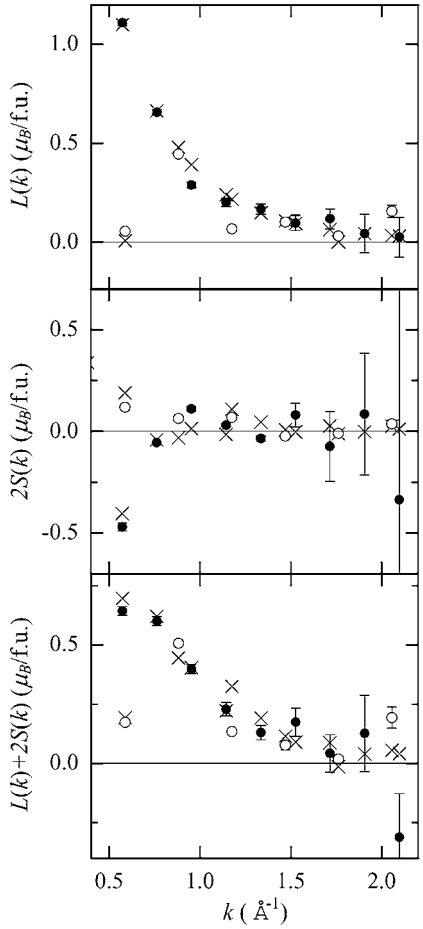

Figure 5. Magnetic form factors, $S(k)$, $L(k)$ and $L(k)+2S(k)$, calculated from observed R-values using equation (1). The results for the reflection series (h h 0) are shown as filled circles from (6 6 0) to (22 22 0), and the results for the ($3h$ $3h$ h) series are shown as open circles from (6 6 2) to (21 21 7). The results of the fitting are also shown as crosses for both reflection groups.

values of R for (2 2 0) are thought to be unreliable judging from their asymmetric distribution of R in figure 3. One of the reasons for the asymmetric distribution can be provided by the following arguments. In the measurements of the (h h 0) reflection series, the angle between the incident (or scattered) x-rays and the plane of the surface of the sample is as small as 9.8°. The absorption effect at the energy of 3.34 keV on the (2 2 0) peak, which strongly depends on the roughness of the surface of the sample, is much larger than that on the other higher-energy peaks. Therefore, the small movement of the sample can have a considerable influence on the absorption effects on the (2 2 0) intensity when the electromagnet switches the direction of the external field. The values of $\langle j_0 \rangle_{\mathrm{M}}$ and $\langle j_2 \rangle_{\mathrm{M}}$ are quoted from [32], where the values for Sm are based on a single J-state. The dependence of the shape of the magnetic form factors on the J-state is estimated to be small, so the possibility of excited J-states has no appreciable effect on our analysis. The values of S_{Sm}, L_{Sm}, S_{Fe}, L_{Fe} obtained are tabulated in table 2. $S(k)$, $L(k)$, and $L(k)+2S(k)$ deduced using the values of S_{Sm}, L_{Sm}, S_{Fe}, L_{Fe} from the fitting are plotted in figure 5. The values obtained by analysis are in favourable agreement with the measured ones

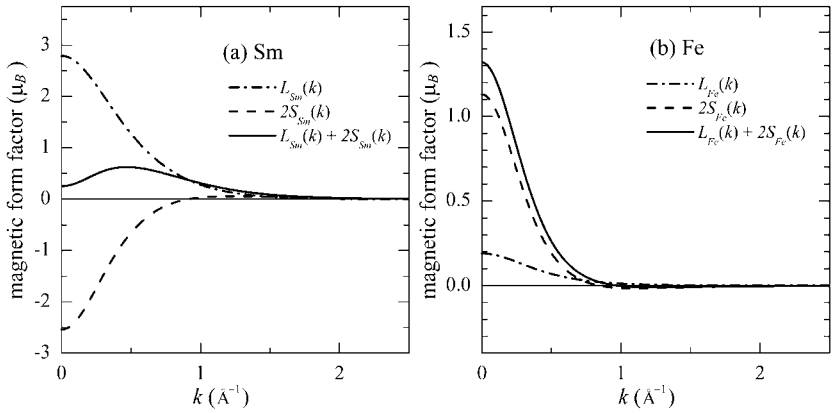

Figure 6. Magnetic form factors $S(k)$, $L(k)$, and $L(k) + 2S(k)$ estimated from the values from the analysis of the fitting (a) for Sm, (b) for Fe.

Table 2. Spin and orbital magnetic moments which have been obtained by a fitting based on the dipole approximation. The total magnetization $L + 2S$ per unit formula for $SmFe_2$ is also tabulated.

	Sm ion	Fe ion	$SmFe_2$
L (μ_B)	2.79 (±0.61)	0.19 (±0.04)	
$2S$ (μ_B)	−2.54 (±0.55)	1.13 (±0.25)	
$L + 2S$ (μ_B)	0.25	1.32	2.89

as seen in figure 5. The magnetic form factors calculated from the results of the fitting are shown in figures 6(a) and (b) for Sm and Fe, respectively. There are three possible sources of errors in the values of the moments in table 2. The first one is the statistical error represented as the square of photon counts. The second is the systematic error due to the inherent noises in the electronic devices or the instability of the polarization factor during the experiments. The third error is in the fitting analysis of the least-squares method. Among these, the most significant error is the statistical one, dominating over the systematic and the fitting errors.

The total magnetic moment of $SmFe_2$, 2.89 μ_B per formula unit, is slightly larger than the value 2.60 μ_B (at 1 T) estimated from the magnetization. One of the reasons is that the direction of the spin polarization of the conduction electrons is opposite to that of the external field, and this contribution cannot be probed by the present diffraction study. The orbital magnetic moment of the Fe ion was estimated to be 0.19 μ_B which is twice that of a pure iron metal and is parallel to the spin magnetic moment. The spin and the orbital moments of Sm ions are both large and couple with an antiparallel configuration. The cancellation of L and $2S$ for Sm reduces the total magnetization to 0.25 μ_B, which is much smaller than the value expected from Hund's rule, 0.71 μ_B. It is known that Sm has a J-mixing state, where both the first excited state of the J-multiplets and the ground state are mixed with each other because the gap of these states is so small [26, 27]. This peculiar magnetism of Sm may reduce the magnetic moments at the Sm site in $SmFe_2$. The present result also shows that there is an antiparallel coupling of the spin magnetic moments between Fe sites and Sm sites, which is consistent with the theory of 3d–4f interaction.

4. Conclusions

WXMD in $SmFe_2$ was measured for the reflection series $(h\ h\ 0)$ and $(3h\ 3h\ h)$. The magnetic form factors have been successfully separated into the spin and the orbital components. The spin and the orbital magnetic moments were estimated for Sm and Fe atoms by a least-squares fitting based on the dipole approximation. The spin and the orbital moments of Sm ions were deduced as $2.79\pm0.61\ \mu_B$ and $-2.54\pm0.55\ \mu_B$, respectively. The antiparallel coupling of these moments leads to the small amount of total magnetization at the Sm site. It was clearly shown that the spin moment of the Fe ions, $1.13 \pm 0.25\ \mu_B$, was dominant in the total magnetization of $SmFe_2$, where the orbital moment of the Fe ions is $0.19 \pm 0.04\ \mu_B$ in the direction parallel to the spin moment.

Acknowledgments

This work was performed with the approval of the Photon Factory Programme Advisory Committee (Proposal No 97S1-001). The authors would like to acknowledge Mr T Tominaga for his experimental help. This work was partially supported by a Grant-in-Aid for Scientific Research from the Japanese Ministry of Education, Science, Sports and Culture.

References

[1] de Bergevin F and Brunel M 1972 *Phys. Lett.* A **39** 141
[2] Platzman P M and Tzoar N 1970 *Phys. Rev.* B **2** 3556
[3] Blume M and Gibbs D 1988 *Phys. Rev.* B **37** 1779
[4] Lovesey S W 1987 *J. Phys. C: Solid State Phys.* **20** 5625
[5] Ito M, Itoh F, Tanaka Y, Koizumi A, Sakurai H, Ohata T, Mori K, Ochiai A and Kawata H 1995 *J. Phys. Soc. Japan* **64** 2333
[6] Fernandez V, Vettier C, de Bergevin F, Giles C and Neubeck W 1998 *Phys. Rev.* B **57** 7870
Neubeck W, Vettier C, Fernandez V, de Bergevin F and Giles C 1999 *J. Appl. Phys.* **85** 4847
[7] Gibbs D, Grubel G and Harshman D R 1991 *Phys. Rev.* B **43** A5663
[8] Pokatilov V S 1998 *J. Magn. Magn. Mater.* **189** 189
[9] Oppelt A and Buschow K H J 1976 *Phys. Rev.* B **13** 4698
[10] Kennedy S J, Brown P J and Coles B R 1993 *J. Phys.: Condens. Matter* **5** 5169
[11] Brueckel T, Lippert M, Koehler T, Schneider J R, Prandl W, Rilling V and Shilling M 1996 *Acta Crystallogr.* A **52** 427
Strempfer J, Brueckel T, Ruett U, Schneider J R, Liss K-D and Tschentscher T 1996 *Acta Crystallogr.* A **52** 438
[12] Langridge S, Lander G H, Bernhoeft N, Stunault A, Vettier C, Grubel G, Stuffer C, de Bergevin F, Nuttall W J, Stirling W G, Mattenberger K and Vogt O 1997 *Phys. Rev.* B **55** 6392
[13] Durbin S M 1998 *Phys. Rev.* B **57** 7595
[14] Collins S P and Laundy D 1992 *Phil. Mag.* B **65** 37
[15] Laundy D and Collins S P 1991 *J. Phys.: Condens. Matter* **3** 369
[16] Collins S P, Laundy D and Guo G Y 1993 *J. Phys.: Condens. Matter* **5** L637
[17] Zukowski E, Cooper M J, Armstrong R, Ito M, Collins S P, Laundy D and Andrejczuk A 1992 *J. X-ray Sci. Technol.* **3** 300
[18] Ito M, Fujii T, Harumoto M, Sakai N, Hashimoto H, Itoh F, Nakamura T, Nanao S, Kawata H, Mori T, Matsumoto M and Wakoh S 1996 *Photon Factory Activity Report* No 14 p 46
[19] Ito M, Harumoto M, Miyagawa H, Nakamura T, Watanabe Y, Nanao S, Adachi H, Mori T, Kawata H and Tanaka Y 1997 *Photon Factory Activity Report* No 15 p 131
[20] Ito M, Fujii T, Harumoto M, Nakamura T, Mori T, Murakami Y and Kawata H 1996 *Photon Factory Activity Report* No 14 p 48
[21] Nakamura T, Ito M, Fujii T, Harumoto M, Katayama T and Nanao S 2002 in preparation
[22] Buschow K H J and van Stapele R P 1971 *J. Physique Coll. Suppl. 2–3* **32** C1 672
[23] Dublon G, Dariel M P and Atzmony U 1975 *Phys. Lett.* A **51** 262
[24] Clark A E 1980 *Ferromagnetic Materials* vol 1, ed E P Wohlfarth (Amsterdam: North-Holland) p 556

[25] Samata H, Fujiwara N, Nagata Y, Uchida T and Der Lan M 1998 *Japan. J. Appl. Phys.* **37** 5544
[26] De Wijn H W, Van Diepen A M and Buschow K H J 1976 *Phys. Status Solidi* b **76** 11
De Wijn H W, van Diepen A M and Buschow K H J 1973 *Phys. Rev.* B **7** 524
[27] Malik S K and Vijayaraghavan R 1974 *Phys. Rev.* B **10** 283
[28] Koehler W C and Moon R M 1972 *Phys. Rev. Lett.* **29** 1468
[29] Brunel M and de Bergevin F 1981 *Acta Crystallogr.* A **37** 324
[30] Blume M 1985 *J. Appl. Phys.* **57** 3615
[31] Balcar E and Lovesey S W (ed) 1989 *Theory of Magnetic Neutron and Photon Scattering* (Oxford: Oxford University Press) p 29
[32] 1992 *International Tables for X-Ray Crystallography* ed A J C Wilson (Dordrecht: IUCr/Kluwer)
[33] Sakai N and Ohno K 1976 *Phys. Rev. Lett.* **37** 351
[34] Cooper M J, Laundy D, Cardwell D A, Timms D N and Holt R S 1986 *Phys. Rev.* B **34** 5984
[35] Collins S P, Cooper M J, Timms D, Brahmia A, Laundy D and Kane P P 1989 *J. Phys.: Condens. Matter* **1** 9009